New Phytologist

Research

The nature of the CO_2-concentrating mechanisms in a marine diatom, *Thalassiosira pseudonana*

Romain Clement[1], Laura Dimnet[1], Stephen C. Maberly[2] and Brigitte Gontero[1]

[1]Aix-Marseille Université CNRS, BIP UMR 7281, 31 Chemin Joseph Aiguier, Marseille Cedex 20 13402, France; [2]Centre for Ecology & Hydrology, Lake Ecosystems Group, Lancaster Environment Centre, Library Avenue, Bailrigg, Lancaster, LA1 4AP, UK

Author for correspondence:
Brigitte Gontero
Tel: +33 4 91 16 45 49
Email: bmeunier@imm.cnrs.fr

Received: *11 July 2015*
Accepted: *25 September 2015*

New Phytologist (2016) **209:** 1417–1427
doi: 10.1111/nph.13728

Key words: Bicarbonate use, carbon dioxide-concentrating mechanism (CCM), CO_2, diatom, photosynthesis, *Thalassiosira pseudonana*.

Summary

- Diatoms are widespread in aquatic ecosystems where they may be limited by the supply of inorganic carbon. Their carbon dioxide-concentrating mechanisms (CCMs) involving transporters and carbonic anhydrases (CAs) are well known, but the contribution of a biochemical CCM involving C_4 metabolism is contentious.
- The CCM(s) present in the marine-centric diatom, *Thalassiosira pseudonana*, were studied in cells exposed to high or low concentrations of CO_2, using a range of approaches.
- At low CO_2, cells possessed a CCM based on active uptake of CO_2 (70% contribution) and bicarbonate, while at high CO_2, cells were restricted to CO_2. CA was highly and rapidly activated on transfer to low CO_2 and played a key role because inhibition of external CA produced uptake kinetics similar to cells grown at high CO_2. The activities of phosphoenolpyruvate (PEP) carboxylase (PEPC) and the PEP-regenerating enzyme, pyruvate phosphate dikinase (PPDK), were lower in cells grown at low than at high CO_2. The ratios of PEPC and PPDK to ribulose bisphosphate carboxylase were substantially lower than 1, even at low CO_2.
- Our data suggest that the kinetic properties of this species results from a biophysical CCM and not from C_4 type metabolism.

Introduction

Diatoms are unicellular microalgae that appeared *c.* 120–250 million yr ago (Sims *et al.*, 2006; Sorhannus, 2007) and have since evolved to form a group of 30 000–100 000 species (Mann & Vanormelingen, 2013) that are ubiquitous in aquatic and moist habitats. Like other Chromista, diatoms are thought to be derived from endosymbioses between a heterotrophic cell, a red alga, and possibly a genetic contribution from a green alga (Armbrust, 2009; Moustafa *et al.*, 2009; Deschamps & Moreira, 2012). Because of their complex evolutionary history, the diatom genome comprises genes from algae, as well as animals and bacteria. This confers diatoms with features, such as the presence of the urea cycle, that differentiate them from other photoautotrophs (Allen *et al.*, 2011). This biochemical diversity could be linked to their ecological success, as the dominant oceanic phytoplankton switched from cyanobacteria and green algae to Chromista, such as diatoms and haptophytes, (Falkowski *et al.*, 2004) at a time when atmospheric CO_2 concentration declined and O_2 concentration increased (Katz *et al.*, 2005; Armbrust, 2009; Raven *et al.*, 2012). Today, diatoms are responsible for up to 40% of primary production in the Earth's largest ecosystem, the ocean (Roberts *et al.*, 2007a), and a large proportion of the export of organic carbon to the ocean floor (Sarthou *et al.*, 2005).

Ribulose-1,5-biphosphate carboxylase/oxygenase (Rubisco) is universally present in photosynthetic organisms and catalyses two reactions, a carboxylation of ribulose-1,5-bisphosphate (RuBP) with CO_2, and an oxygenation of RuBP with O_2 (Bowes *et al.*, 1971; Gontero & Salvucci, 2014). These two reactions compete and thus the oxygenase reaction is favoured at low CO_2 concentrations, reducing photosynthesis (Badger *et al.*, 1998). The Michaelis–Menten constant (K_m) for CO_2 of Rubisco of diatoms varies from 20 to 60 μM, which is higher than the CO_2 concentration in marine ecosystems at equilibrium with the current atmosphere of 400 ppm (*c.* 16 μM depending on temperature; Badger *et al.*, 1998; Whitney *et al.*, 2011). To circumvent or reduce carbon limitation of photosynthesis, some aquatic photosynthetic organisms, including diatoms, possess carbon dioxide-concentrating mechanisms (CCMs) that elevate the CO_2 concentration around Rubisco, thus decreasing the oxygenase reaction and thereby increasing the rate of photosynthesis (Roberts *et al.*, 2007a).

Several types of CCM are known, based on biophysical or biochemical processes. Biophysical CCMs involve active transport of CO_2 or bicarbonate (HCO_3^-), and are present in many diatoms (Matsuda *et al.*, 2011). For instance, in marine diatoms, the SLC4 HCO_3^- transporter is present in *Phaeodactylum tricornutum* (Nakajima *et al.*, 2013), and homologous encoding genes are also found in *Thalassiosira pseudonana* (Armbrust *et al.*, 2004). Carbonic anhydrase (CA) maintains equilibrium between CO_2 and HCO_3^- by catalysing the reversible interconversion of CO_2 and water into HCO_3^- and protons. It plays a role in

diatom CCMs (Hopkinson *et al.*, 2011; Matsuda *et al.*, 2011) and its expression is increased under a low CO_2 concentration in *P. tricornutum* and *T. pseudonana* (Harada *et al.*, 2005; Crawfurd *et al.*, 2011; Hopkinson *et al.*, 2013). In *P. tricornutum*, some CAs are redox-regulated and activated by reduced thioredoxins, suggesting that they are active during the day and inactive at night, which is consistent with their participation in a CCM (Kikutani *et al.*, 2012).

Biochemical CCMs involving C_4-type photosynthesis have been suggested to be involved in CO_2 assimilation in some diatoms (Reinfelder *et al.*, 2000). A functional C_4 CCM requires an additional carboxylation enzyme, typically phosphoenolpyruvate carboxylase (PEPC), which catalyses the carboxylation of phosphoenolpyruvate (PEP) with HCO_3^-, forming a C_4 carbon compound. This compound is then cleaved by one of three decarboxylating enzymes to produce CO_2 in the vicinity of Rubisco (Sage, 2004). Although C_4 metabolism in terrestrial plants is usually associated with Kranz-type anatomy (Sage, 2004), some terrestrial plants, such as *Borszczowia aralocaspica*, perform C_4-type photosynthesis within one cell (Voznesenskaya *et al.*, 2001). Similarly, in aquatic environments, *Hydrilla verticillata*, *Ottelia alismoides*, *Egeria densa*, *Udotea flabellum* and *Ulva lynza* are believed to perform this type of photosynthesis without Kranz anatomy (Reiskind & Bowes, 1991; Magnin *et al.*, 1997; Lara *et al.*, 2002; Xu *et al.*, 2013; Zhang *et al.*, 2014) and so it is feasible that this pathway may be present in diatoms (Kroth, 2015).

In two diatoms whose genomes are fully sequenced and annotated, *T. pseudonana* (Armbrust *et al.*, 2004) and *P. tricornutum* (Bowler *et al.*, 2008), all the genes required for C_4-type photosynthesis are present. Thus, diatoms have the genetic potential to operate a C_4 pathway. However, this possibility remains controversial (Raven, 2010) as there are a range of contradictory results for the possession of C_4 metabolism in diatoms based on different approaches such as ^{14}C labelling, use of specific C_4 enzyme inhibitors (Reinfelder *et al.*, 2004), proteomic analysis, transcriptomic analysis, enzyme localization and RNA silencing (McGinn & Morel, 2008; Kustka *et al.*, 2014; Tanaka *et al.*, 2014). A recent study (Kustka *et al.*, 2014), however, reaffirmed the operation of C_4 photosynthesis in *T. pseudonana* grown at low CO_2 and concluded that the nature of the CO_2 delivery system to the chloroplast needs to be investigated further (Samukawa *et al.*, 2014).

The aim of this study was therefore to decipher the roles of biophysical and biochemical CCMs in a model diatom, *T. pseudonana*, using a range of techniques. We studied the effect of growth in air (400 ppm CO_2) and extremely high (20 000 ppm) and low (50 ppm CO_2) on growth rate, photosynthetic kinetics, the activity of CA and the enzymes involved in C_4-type metabolism.

Materials and Methods

Strain, media and culture condition

Thalassiosira pseudonana Hasle & Heim., strain CCAP 1085/12 (equivalent to CCMP1335, the strain whose genome has been sequenced), was grown in F/2 + Si medium, pH 8, in artificial sea water (mM: 380 NaCl, 3 KCl, 4.39 $CaCl_2$, 1.71 $NaHCO_3$, 20.8 $MgSO_4$, 0.88 $NaNO_3$, 0.036 NaH_2PO_4, 0.11 Na_2SiO_3), trace elements (μM: 12.3 Na_2EDTA, 11.7 $FeCl_3$, 40.1 $CuSO_4$, 0.077 $ZnSO_4$, 0.042 $CoCl_2$, 0.91 $MnCl_2$, 0.013 Na_2Mo_4,) and vitamins (nM: 0.37 B12 (cyanocobalamin), 300 B1 (thiamine-HCl) and 2.05 B8 (biotin)).

Cultures were maintained in a growth cabinet (Innova 4230; New Brunswick Scientific, Edison, NJ, USA) at 16°C with continuous illumination at 50 μmol photon m^{-2} s^{-1} photosynthetically active radiation (PAR, spectral band 400–700 nm) measured with a 2π sensor (Q201; Macam Photometric, Livingstone, UK) and were constantly shaken at 90 rpm. The cultures were aerated with one of three gas mixtures (50, 400 or 20 000 ppm) at a gas flow rate of 130 ml min^{-1} using mass-flow regulators (El-Flow; Bronkhorst High-Tech BT, Nijverheidsstraat, the Netherlands) that mixed air, 2% CO_2 in air, and air that had been passed through soda lime, to remove CO_2 (Intersurgical, Wokingham, UK). Dissolved CO_2 concentrations calculated using equations in Weiss (1974) were 2, 16 and 800 μM. Concentrations of CO_2 and other components of the carbonate system were calculated from pH, alkalinity, temperature and salinity using the dissociation constants in Goyet & Poisson (1989). During growth experiments, pH was checked daily using a combination pH electrode and meter (Eutech pH 2700; Eutech Instruments, Landsmeer, the Netherlands), optical density (OD) was measured at 600 nm using a Perkin Elmer Lambda 25 UV/VIS spectrophotometer (Waltham, MA, USA) and number of cells was counted by microscopy using a Neubauer chamber (Brand GmH, Wertheim, Germany). Growth rates were calculated as:

$$\text{Growth rate} = \left(\frac{\log_e(y_B) - \log_e(y_A)}{x_B - x_A}\right) \qquad \text{Eqn 1}$$

where $\log_e(y_B)$ and $\log_e(y_A)$ correspond to the natural logarithm of OD at 600 nm or cell density (cell ml^{-1}) measured at the start and end of the exponential phase and x_B and x_A correspond to the time (day) of these two points.

Kinetics of O_2 evolution

Rates of net photosynthesis were measured as oxygen evolution in an electrode chamber thermostatted at 16°C (Oxygraph; Hansatech Instruments, Norfolk, UK) using O_2 View software (Hansatech, Norfolk, UK). The chamber was illuminated with a tungsten lamp with a hot-mirror cutoff filter at 750–1100 nm (HMC-1033; UQG (Optics), Cambridge, UK) to minimize heat input to the chamber. The cells received 200 μmol m^{-2} s^{-1} PAR, which preliminary experiments had shown to be saturating but not photoinhibiting. Cultures from the exponential phase were centrifuged at 3720 ***g*** for 10 min at 16°C (Beckman Coulter Allegra® X-15R Centrifuge (Pasadena, CA, USA); rotor: 4750A) and the pellet was rinsed twice, and resuspended in artificial sea water containing 10 mM HEPES at either pH 7 or pH 8. A suspension (1 ml) containing ± 20 million cells was added to the oxygen electrode chamber. Respiration was measured after 10 min in the dark to allow steady-state rates to be produced. The cells were

then illuminated and when net oxygen evolution had ceased, small volumes of stock (1, 10 and 100 mM) $NaHCO_3$ were added to produce a range of concentrations of dissolved inorganic carbon (DIC; 10, 20, 50, 100, 150, 200, 500, 1000 and 2000 μM) and the rate of change of oxygen concentration was recorded. To study the effect of CA on the rate of photosynthesis, 0.4 mM (final concentration) of acetazolamide (AZA; Sigma-Aldrich), an inhibitor of external CA, was added directly to the oxygen electrode in the light once oxygen evolution had ceased and immediately before the first addition of DIC. Biological duplicates and experimental triplicates were analysed, giving six replicates in total. The response of rate of net photosynthesis to the concentration of DIC was fitted to a slightly modified Michaelis–Menten equation that took into account the compensation point for DIC.

At pH 7, CO_2 represents 8% of DIC, while at pH 8 it only represents 0.8%. This difference was used to discriminate between the effects of CO_2 and HCO_3^- on net oxygen evolution using a model that assumes separate uptake of these two forms of inorganic carbon with different $K_{½}$ and compensation concentrations but a common total maximum uptake rate:

$$\text{Net rate of photosynthesis} = \left(\frac{\alpha \times V_{net}^{max} \times (CO_2 - CP^C)}{K_{1/2}^C + (CO_2 - CP^C)}\right) + \left(\frac{(1-\alpha) \times V_{net}^{max} \times (HCO_3^- - CP^B)}{K_{1/2}^B + (HCO_3^- - CP^B)}\right) \quad \text{Eqn 2}$$

where (rate as μmol O_2 mg^{-1} Chl*a* h^{-1} and concentration as μmol l^{-1}) V_{net}^{max} is the maximum rate of net photosynthesis; α is the proportion of V_{net}^{max} resulting from CO_2 uptake; CO_2 is the concentration of CO_2; CP^C is the CO_2 compensation concentration; $K_{1/2}^C$ is the concentration of CO_2 yielding half-maximal rates of net photosynthesis; HCO_3^- is the concentration of HCO_3^-; CP^B is the HCO_3^- compensation concentration; and $K_{1/2}^B$ is the concentration of HCO_3^- yielding half-maximal rates of net photosynthesis.

The best fit of the model parameters to the data was obtained by minimizing the residual sum of squares of the difference between the measured and modelled rates of net photosynthesis.

Chlorophyll extraction and measurement

The culture was centrifuged at 3720 ***g***, for 10 min at 4°C. The pellet was rinsed in distilled water and re-centrifuged, and 2 ml of 96% ethanol was added. After incubation for 15 min at 4°C in the dark, the supernatant was removed and a second extraction was performed. The optical density of the bulked supernatant was measured with the spectrophotometer at 629 and 665 nm. Optical density at 750 nm was negligible and so uncorrected values were used to calculate concentrations of Chl*a* using the equation in Ritchie (2006):

$$\text{Chl}\,a\ (\mu g\,ml^{-1}) = -1.4014 \times A629 + 12.1551 \times A665. \quad \text{Eqn 3}$$

Protein extraction and content

The soluble protein extracts were prepared as described previously (Erales *et al.*, 2008; Mekhalfi *et al.*, 2014) in a buffer containing 1 mM NAD. The soluble protein concentration of crude extracts was assayed using the Bio-Rad (Hercules, CA, USA) reagent using BSA as a standard (Bradford, 1976).

Enzyme activity measurement

All enzyme activities were measured on cells from the exponential phase of growth. CA activity was measured spectrophotometrically using bromothymol blue as a pH indicator. Crude extracts of cells were incubated in 1.6 ml of buffer (25 mM Tris, 6.4 μM bromothymol blue at pH 9.1) in a cuvette at 3°C. The reaction was started by adding 0.4 ml of CO_2-saturated milliQ water that had been kept on ice. Blanks were performed for each assay by omitting the sample. CA activity was estimated from the time required for the disappearance of the bromothymol blue absorbance at 620 nm which corresponds to a pH decrease from 9.1 to 6.2. Enzyme activity was calculated in Wilbur-Anderson Units (WAU) using the equation (Wilbur & Anderson, 1948):

$$WAU = T_0/T_1 - 1 \quad \text{Eqn 4}$$

where T_0 and T_1 correspond to the acidification time without (blank) and with the sample in the reaction mixture, respectively. External CA (eCA) was determined on intact cells; total CA was determined on cells that had been broken by sonicating (Erales *et al.*, 2008); internal CA (iCA) was calculated from the difference between total CA and eCA.

Other enzyme activities were measured from the rate of appearance or disappearance of NADH or NADPH at 340 nm at room temperature (20–25°C). All biochemicals were obtained from Sigma. PEPC, NAD-dependent malic enzyme (NAD-ME) and pyruvate phosphate dikinase (PPDK) activities were measured as described previously (Zhang *et al.*, 2014). The activities of fully CO_2-activated and nonactivated Rubisco were measured. To activate Rubisco, the extract was preincubated in 50 mM Tris, 0.1 mM EDTA, 15 mM $MgCl_2$, 40 mM bicarbonate and 5 mM dithiothreitol, pH 8.0, for 10 min before assay in a 1 ml cuvette. To measure activity, five units of phosphoglycerate kinase and glyceraldehyde-3-phosphate dehydrogenase, 1 mM ATP and 0.2 mM NADH were added and the reaction was started by adding 1 mM ribulose 1,5-bisphosphate. The activity of nonactivated Rubisco was measured as described earlier, but the reagents were all added at the same time without preincubation. The activation procedure is equivalent to that used to carbamylate Rubisco in higher plants, cyanobacteria and a range of algae, but whether or not this is the mechanism involved in activation has not, to our knowledge, been studied in diatoms.

Rubisco, PEPC and CA activities were measured as a function of time after the switch to low CO_2, and the curves were fitted with SIGMA PLOT software (Systat Software GmbH, Erkrath, Germany) to experimental data using Eqn 5 for the carboxylases, and their activity ratio and Eqn 6 for CA:

$$A = A_0 + p(1) \times (e^{-p(2) \times t}) \quad \text{Eqn 5}$$

and

$$A = A_0 + p(1) \times (1 - e^{-p(2) \times t}) \quad \text{Eqn 6}$$

where A is the rate of reaction mg^{-1} of Chl*a*, A_0 is the activity at the beginning of the experiment before the switch to low CO_2, $p(1)$ is the amplitude and $p(2)$ is the time constant.

Statistical analysis

Results were analysed using SIGMA PLOT (v.11.0).

Results

Effect of CO_2 on growth rate

The growth rate of *T. pseudonana*, was determined at three concentrations of CO_2. In the absence of algae, the pH values at equilibrium with 50, 400 and 20 000 ppm CO_2 were 8.8, 7.9 and 6.7, respectively. The corresponding calculated CO_2 concentrations were 1, 19 and 320 μM for 50, 400 and 20 000 ppm, respectively, which were similar to the theoretical concentrations apart from at the highest CO_2 concentration. In the cultures with algae at 20 000 ppm, the pH dropped quickly to 6.9 and then remained constant for several days (Fig. 1b). During exponential growth, the geometric mean pH was 6.95, equivalent to a CO_2 concentration of *c.* 180 μM. At 400 ppm, pH increased progressively during the exponential phase and reached up to pH 9–9.2 at the beginning of the stationary phase. The geometric average pH during the exponential phase was 8.55, which is equivalent to a CO_2 concentration of *c.* 3 μM. Similarly, when the cells were shifted from 20 000 to 50 ppm, the pH also increased and reached over 9.5, corresponding to < 0.1 μM CO_2 (Fig. 1b). These elevated pH values were caused by the rate of CO_2 consumption at high cell density exceeding the rate of CO_2 supply. The maximum specific growth rate ($0.70 \pm 0.01\ d^{-1}$) at 20 000 ppm CO_2 was *c.* 1.3-fold higher than at 400 ppm CO_2 ($0.54 \pm 0.02\ d^{-1}$, Fig. 1a). A similar ratio of growth rate at high and ambient CO_2 was found, based on cell counts (data not shown). *T. pseudonana* was unable to grow when transferred from 20 000 to 50 ppm (Fig. 1a). As the pH in the 50 ppm treatment was stable for several days, it indicates that the treatment was not so severe as to cause cell death and this is consistent with the optical density data (Fig. 1a).

Photosynthetic activity

The maximal rate of net photosynthesis (V_{net}^{max}) of *T. pseudonana* grown under 400 ppm CO_2 and measured at pH 7 (*c.* 110 μmol O_2 h^{-1} mg^{-1} Chl*a*) was similar to that measured at pH 8 (Fig. 2a; Table 1). By contrast, the half-saturation concentration for DIC at pH 7 was *c.* threefold lower than that at pH 8 (Table 1). The DIC compensation point was also threefold lower at pH 7 than at pH 8. For cells grown at 20 000 ppm CO_2, the maximal photosynthetic activity (V_{net}^{max}) measured at pH 7 was *c.* 205 μmol O_2 h^{-1} mg^{-1} Chl*a*, which was twice that measured at pH 8 (Fig. 2d, Table 1). The half-saturation concentrations for DIC at pH 7 and pH 8, by contrast, were rather similar and *c.* 50 μM. The DIC compensation points were 3 and 5 μM at the two pH values. When *T. pseudonana* was grown at 20 000 ppm CO_2, the slope of rate of photosynthesis against DIC was between 3.5 and 6.5-fold lower than that found when *T. pseudonana* was grown at 400 ppm CO_2 (Table 1).

The different kinetic parameters at pH 7 and 8 are consistent with different proportions of CO_2 and HCO_3^- being present at these two pH values and we used this to develop a model that distinguished between CO_2 and HCO_3^- uptake (Eqn 2). For cells grown at 400 ppm, this model gave a good fit to the data (R^2 of 0.92; Table 2) and a V_{net}^{max} of 112 μmol O_2 h^{-1} mg^{-1} Chl*a*, corresponding to the sum of CO_2- and HCO_3^--dependent uptake, which was similar to that found when modelling kinetics against DIC. The model predicted that at saturation, CO_2 contributed 70% and HCO_3^- contributed 30% to the maximal rate (Fig. 2b, c). The half-saturation concentration for CO_2 was 0.4 μM which was 7.5-fold lower than that for HCO_3^- at 3 μM. The compensation points were close to 0 for CO_2 and 7 μM for HCO_3^-. The slope of uptake was seven times higher for CO_2 than for HCO_3^-.

For cells grown at 20 000 ppm, the model fitted the data less well than at 400 ppm (R^2 of 0.60; Table 2). The V_{net}^{max} for CO_2

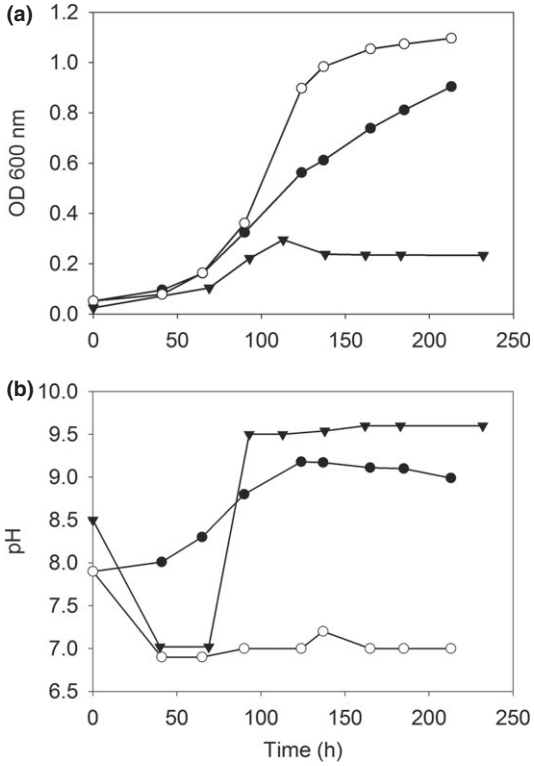

Fig. 1 Growth of *Thalassiosira pseudonana* and pH of culture at 400 ppm CO_2 (closed circles), 20 000 ppm CO_2 (open circles) and then switched from 20 000 to 50 ppm CO_2 after 60 h (triangles). (a) Growth followed using optical density at 600 nm; (b) culture pH.

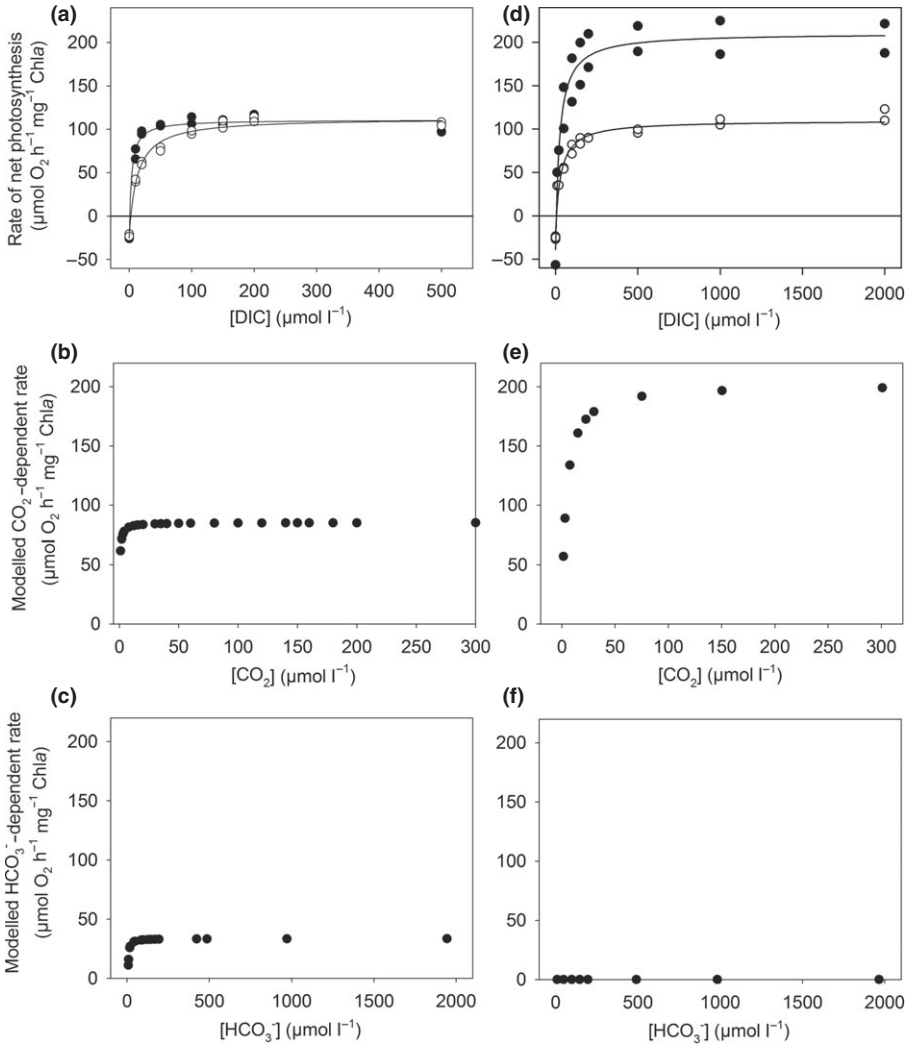

Fig. 2 Rate of net photosynthesis of *Thalassiosira pseudonana* grown at 400 or 20 000 ppm CO_2. (a) Rate measured for 400 ppm cultures at pH 7 (closed circles) or pH 8 (open circles) vs concentration of dissolved inorganic carbon (DIC). (b) Modelled rate for 400 ppm cultures for combined pH values vs concentration of CO_2. (c) Modelled rate for 400 ppm cultures for combined pH values vs concentration of HCO_3^-. (d) Rate measured for 20 000 ppm cultures at pH 7 (closed circles) or pH 8 (open circles) vs concentration of dissolved inorganic carbon. (e) Modelled rate for 20 000 ppm cultures for combined pH values vs concentration of CO_2. (f) Modelled rate for 20 000 ppm cultures for combined pH values vs concentration of HCO_3^-. The kinetic parameters for the model are shown in Table 2.

Table 1 Kinetics of photosynthesis by *Thalassiosira pseudonana* grown at different CO_2 concentrations and measured at different pH values and treated with 0.4 mM acetazolamide (AZA)

CO_2 (ppm)	pH	V_{net}^{max} (μmol O_2 h^{-1} mg^{-1} Chl*a*)	$K_{½}$ (μmol DIC l^{-1})	CP (μmol DIC l^{-1})	Slope (μmol O_2 h^{-1} mg^{-1} Chl*a* μmol^{-1} DIC l)	R^2
400	7	111 (3)	4.2 (0.9)	0.8 (0.2)	26 (6)	0.99
400	8	113 (3)	15.3 (1.6)	2.4 (0.4)	7 (1)	0.99
20 000	7	205 (17)	58.9 (22.6)	2.9 (5.9)	4 (1)	0.74
20 000	8	95 (8)	46.5 (19)	5.1 (4.7)	2 (1)	0.71
50 (6 h)	7	179 (5)	25.3 (3.6)	3.1 (0.9)	7 (1)	0.95
50 (12 h)	7	156 (3)	13.3 (1.4)	1.8 (0.4)	12 (1)	0.97
400 + AZA	7	163 (7)	23.0 (4.2)	3.2 (0.9)	7 (1)	0.96

Values are means with standard error in parentheses.
DIC, dissolved inorganic carbon; V_{net}^{max}, the maximum rate of net photosynthesis; $K_{½}$, half-saturation concentration for DIC; CP, compensation point.

was nearly identical to that of DIC and the contribution of HCO_3^- was zero (Fig. 2e,f; Table 2). The half-saturation concentration for CO_2 was 3.8 μM and the compensation point was again close to 0 for CO_2. In comparison to the cells grown at 400 ppm, cells at 20 000 ppm had a 1.8-fold greater V_{net}^{max}, a nearly 10-fold higher half-saturation constant for CO_2, and thereby a 5.5-fold lower slope against CO_2 and lacked the ability to use HCO_3^-. At ambient conditions, presumed to be 16 μM CO_2 and 2000 μM HCO_3^-, the rate of net photosynthesis was 98% saturated for cells grown at 400 ppm but only 80%

saturated for cells grown at 20 000 ppm (Table 2). For a 10-fold lower CO_2 concentration of 1.6 μM, the rates of net photosynthesis were 81% and 30% saturated for cells grown at 400 and 20 000 ppm, respectively. Ambient concentrations of 2000 μM HCO_3^- were saturating for cells grown at 400 ppm, but HCO_3^- use was absent in cells grown at 20 000 ppm.

Net photosynthetic rate was also measured at pH 7 for cells switched from 20 000 ppm CO_2 to low CO_2 (50 ppm) for 6 or 12 h (Fig. 3). After 6 or 12 h at a low CO_2 concentration, the slopes were lower than that of cells grown at 400 ppm CO_2 concentration. However at pH 7, V_{net}^{max} values were intermediate to those found at 400 and 20 000 ppm, with a tendency to decrease as a function of time (Table 1). The half-saturation constant values also decreased as a function of time (Table 1). However, even after 12 h at 50 ppm, the slope of photosynthesis rate to concentration of DIC was lower than for cells grown for several days at 400 ppm.

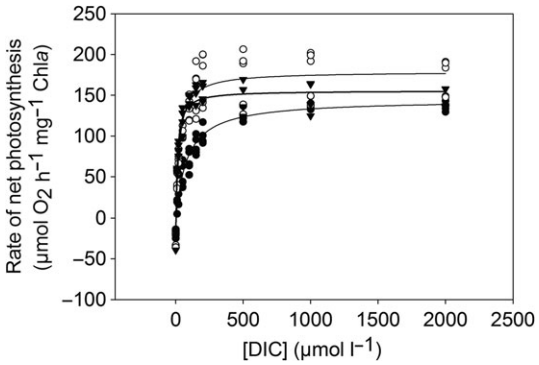

Fig. 3 Rate of net photosynthesis at pH 7 of *Thalassiosira pseudonana* grown at 20 000 ppm CO_2 (closed circles) and then switched to 50 ppm CO_2 for 6 h (open circles) or 12 h (triangles).The experimental data were fitted to a slightly modified Michaelis–Menten equation that took into account the compensation point for dissolved inorganic carbon (DIC); parameters are given in Table 1.

Enzyme activities

Enzymes that could be involved in biochemical or biophysical CCMs in *T. pseudonana* were studied. The activity of Rubisco was lower in cells grown at 400 ppm than in those grown at 20 000 ppm (1.59-fold, Student's *t*-test, $P < 0.001$; Fig. 4). The rates of Rubisco activity (as carbon) cannot account for the oxygen-based rates of photosynthesis (6 vs 100 μmol h^{-1} mg^{-1} Chl*a* at 400 ppm and 20 vs 205 μmol h^{-1} mg^{-1} Chl*a* at 20 000 ppm). The activity of fully CO_2-activated Rubisco was, however, approx. threefold higher than that of nonactivated enzyme, at both 400 (18 μmol h^{-1} mg^{-1} Chl*a*) and 20 000 ppm CO_2 (60 μmol h^{-1} mg^{-1} Chl*a*), but again this was lower than the oxygen-based rates of photosynthesis even after assuming a photosynthetic quotient of 1.26 (Spilling *et al.*, 2015). However, other mechanisms such as activation by protein–protein interaction with, for instance, CbbX may also be involved (Mueller-Cajar *et al.*, 2011). Surprisingly, activities of the C_4 enzymes PEPC and PPDK were also lower (5.3-fold, Student's *t*-test, $P < 0.001$, and 4.6-fold, Student's *t*-test, $P < 0.001$, for PEPC and PPDK, respectively) in cells from 400 ppm than those from 20 000 ppm CO_2. By contrast, in cells grown at 400 ppm, NAD-ME and CA activities were higher (4.3-fold, Student *t*-test, $P < 0.001$, and 3.75-fold, Student *t*-test, $P < 0.001$, respectively) than in cells grown at 20 000 ppm CO_2.

Thalassiosira pseudonana cells acclimated to 20 000 ppm CO_2 were shifted to 50 ppm CO_2 to determine the rate of acclimation and to characterize the CCM under more carbon-limiting conditions. Rubisco and PEPC activities both decreased exponentially with a time constant of 0.086 (0.044) and 0.064 (0.035) h^{-1}, respectively (Fig. 5a). Consequently, the PEPC : Rubisco ratio, which began at *c.* 0.27, also decreased exponentially to reach *c.* 0.07 at 48 h after the switch to low CO_2 (Fig. 5b). Therefore, the PEPC : Rubisco ratios are always much less than 1. At 12 h after the switch to 50 ppm CO_2, the activity of NAD-ME increased 5.6 (1.2)-fold, while that of PPDK decreased 2.4 (0.2)-fold. These data therefore do not support a role for C_4-type photosynthesis in the carbon assimilation of *T. pseudonana.*

By contrast, upon the switch to low CO_2 concentration, CA activity was induced rapidly. The CA activity that was < 300 WAU increased exponentially to reach a modelled value of 4890 (700) WAU (16-fold increase) with a time constant of 0.13 (0.0587) h^{-1} (Fig. 5c). A ratio between iCA and eCA of *c.* 1 was obtained for cells grown at all three CO_2 concentrations. The effect of inhibiting eCA on the net photosynthetic rate of

Table 2 Modelled kinetics of CO_2-dependent and HCO_3^--dependent photosynthesis by *Thalassiosira pseudonana* grown at 400 or 20 000 ppm CO_2

	V_{net}^{max} (μmol mg^{-1} Chl*a* h^{-1})		$K_{½}$ (μmol l^{-1})		CP (μmol l^{-1})		Slope (μmol O_2 h^{-1} mg^{-1} Chl*a* μmol^{-1} l)		% of V_{net}^{max} under ambient		
CO_2 (ppm)	CO_2	HCO_3^-	CO_2	HCO_3^-	CO_2	HCO_3^-	CO_2	HCO_3^-	CO_2	HCO_3^-	R^2
400	85 (9)	27 (9)	0.4 (0.1)	2.7 (0.4)	0.0 (0.0)	7.5 (0.7)	296 (38)	42 (6)	98	100	0.92
20 000	202 (39)	0.0	3.8 (0.1)	–	0.0 (0.0)	–	53 (9)	–	60	–	0.60

Values are means with standard error of the estimate in parenthesis. Estimated rates as a percentage of V_{net}^{max} are calculated for 16 μM CO_2 and 2000 μM HCO_3^-. The raw data are shown in Fig. 2(a,d) and the outcomes of the models are shown in Fig. 2(b,c,e,f).
–, not applicable as bicarbonate use is absent.
V_{net}^{max}, the maximum rate of net photosynthesis; $K_{½}$, half-saturation concentration for DIC; CP, compensation point.

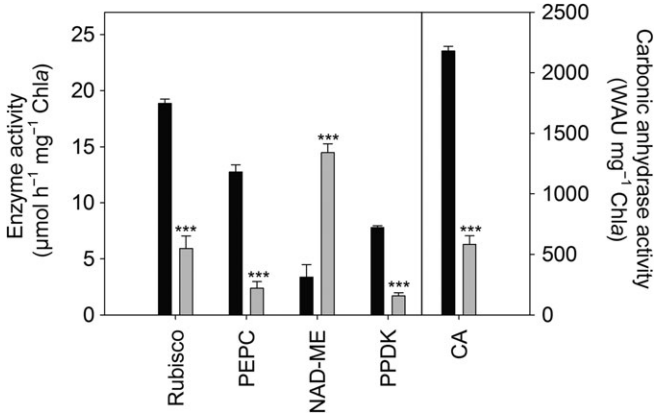

Fig. 4 Activities of partially CO_2-activated Rubisco, C_4 enzymes and carbonic anhydrase (CA) in *Thalassiosira pseudonana* grown at 400 ppm CO_2 (black bars) and 20 000 ppm CO_2 (grey bars). Bars to the left-hand side of the vertical line refer to the left-hand axis, and vice versa. Error bars represent + 1 SD. ***, $P < 0.001$. WAU, Wilbur-Anderson Units; PEPC, phosphoenolpyruvate carboxylase; NAD-ME, NAD-dependent malic enzyme; PPDK, pyruvate phosphate dikinase.

the cells grown at 400 ppm CO_2 was tested at pH 7 using a specific inhibitor of eCA, AZA. The addition of AZA increased the half-saturation constant for DIC fivefold, increased the compensation point *c.* threefold and decreased the slope of response to DIC fourfold, but did not affect the maximum rate of net photosynthesis (Fig. 6; Table 1). The kinetic response of cells grown at 400 ppm CO_2 but treated with AZA resembled those grown at 20 000 ppm CO_2 (Table 1), suggesting that eCA has a key role in the carbon uptake properties of *T. pseudonana.*

In order to check if the response to low CO_2 was reversed on return to high CO_2, cultures grown at 20 000 ppm and switched to 50 ppm for 24 h were then switched back to 20 000 ppm for 12 h. While PEPC and PPDK activity increased (by 4.5-fold, Student's *t*-test, $P < 0.001$, and 5.3-fold, Student's *t*-test, $P < 0.001$, respectively), Rubisco activity did not change. NAD-ME and CA activity decreased (1.4-fold, Student's *t*-test, $P < 0.05$, and 3.3-fold, Student's *t*-test, $P < 0.001$, respectively) (Fig. 7).

These results show that the responses of *T. pseudonana* to CO_2 are rapid and reversible. The kinetic properties of carbon uptake are strongly linked to the activity of CA, and the enzyme activity profiles suggest that carbon fixation involves C_3 rather than C_4 metabolism.

Discussion

Biophysical CCM in *T. pseudonana*

Cells grown at 400 ppm CO_2 have a $K_{½}$ for CO_2 of only 0.4 μM, which is in good agreement with the growth $K_{½}$ estimated for *T. pseudonana* (Clark & Flynn, 2000) at 273 μM DIC, equivalent to *c.* 1.4 μM CO_2 under their experimental conditions. Both estimates are substantially lower than the $K_{½}$ for diatom 1D Rubisco (20–60 μM) (Whitney *et al.*, 2011), which clearly indicates that some form of CCM is operating. *T. pseudonana* grown

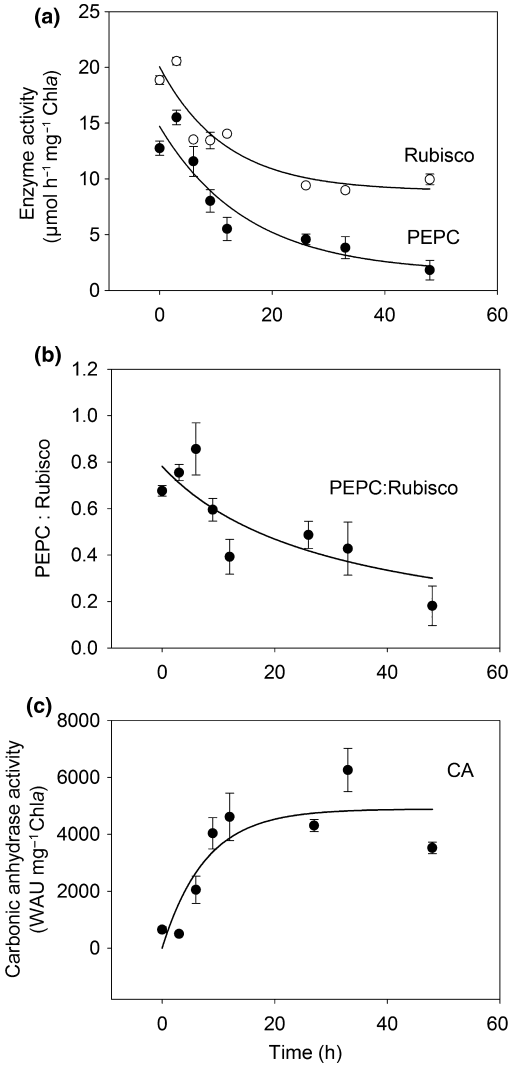

Fig. 5 Time course of enzyme activities after switching cultures from 20 000 ppm to 50 ppm CO_2. (a) Activities of partially CO_2-activated Rubisco (open circles) and PEP carboxylase (PEPC; closed circles). (b) Ratio of PEPC : Rubisco. (c) Activity of carbonic anhydrase (CA). Error bars represent ± 1 SD. WAU, Wilbur-Anderson Units.

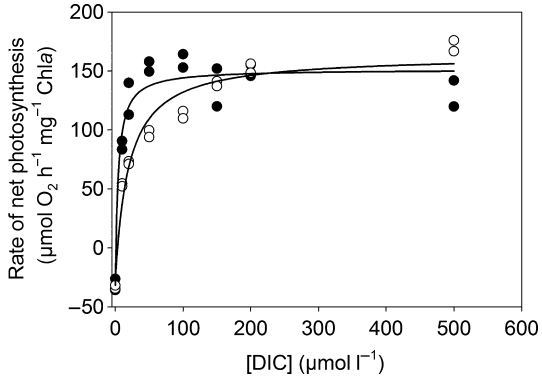

Fig. 6 Effect of acetazolamide (AZA; 0.4 mM) on the kinetics of carbon uptake at pH 7 for *Thalassiosira pseudonana* grown at 400 ppm CO_2. Control (closed circles) and treated cells (open circles) are shown.

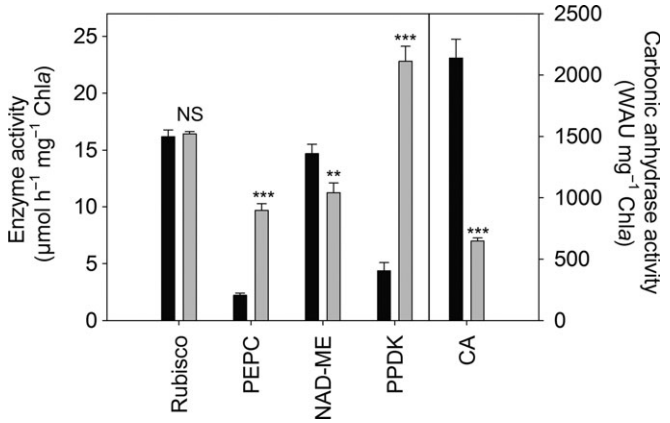

Fig. 7 Activities of partially CO_2-activated Rubisco, C_4 enzymes and carbonic anhydrase (CA) in *Thalassiosira pseudonana* grown at 20 000 ppm CO_2 and switched to 50 ppm CO_2 for 24 h (black bars) and then returned to 20 000 ppm CO_2 for 12 h (grey bars). Bars to the left-hand side of the vertical line refer to the left-hand axis and vice versa. Error bars represent + 1 SD. NS, not significant; **, $P < 0.01$; ***, $P < 0.001$. WAU, Wilbur-Anderson Units; PEPC, phosphoenolpyruvate carboxylase; NAD-ME, NAD-dependent malic enzyme; PPDK, pyruvate phosphate dikinase.

at 400 ppm CO_2 preferentially used CO_2 (70%) rather than HCO_3^- (30%) at ambient and saturating conditions despite the *c.* 120-fold higher concentration of HCO_3^-. This is similar to *P. tricornutum* (Burkhardt *et al.*, 2001) but different from *Thalassiosira weissflogii*, which took up CO_2 and HCO_3^- at a similar rate (Burkhardt *et al.*, 2001). For cells grown at 400 ppm, our reported $K_{½}$ for DIC at pH 8 and 16°C is very similar to that obtained for the same species at pH 8.2 and 20°C (Nakajima *et al.*, 2013) and to that reported for low CO_2-grown *Chlamydomonas reinhardtii* cells (Sültemeyer *et al.*, 1988).

Cells of *T. pseudonana* grown at a 20 000 ppm CO_2 were only able to use CO_2 and the affinity ($K_{½}$) for DIC was over fivefold lower than for cells grown at 400 ppm CO_2, a down-regulation that has been reported in this and other marine diatoms (e.g. Burkhardt *et al.*, 2001; Trimborn *et al.*, 2009; Nakajima *et al.*, 2013) and *C. reinhardtii* (Sültemeyer *et al.*, 1988). In *T. pseudonana*, the $K_{½}$ for CO_2 was still *c.* 4 μM and so substantially lower than the $K_{½}$ value for Rubisco: some down-regulated form of CCM, therefore, still seems to be operating in *T. pseudonana* grown at 20 000 ppm. External and internal CA activity was also still present in these cells, which might be adequate to promote CO_2 uptake – this is consistent with the finding that some forms of CA are constitutive in this species (Samukawa *et al.*, 2014).

Carbonic anhydrase appears to be crucial in this CCM and that of other marine diatoms (Hopkinson *et al.*, 2011). Our enzymatic activity data showing a rapid fourfold up-regulation at 400 vs 20 000 ppm are similar to previous reports (Hopkinson *et al.*, 2013) and also in agreement with data obtained at the transcriptional level (McGinn & Morel, 2008; Kustka *et al.*, 2014; Samukawa *et al.*, 2014). All these reports indicate an increase in CA under low CO_2. In *T. pseudonana*, CA is present in the periplasmic space, cytosol, mitochondria, periplastidial compartment and stroma (Tanaka *et al.*, 2005; Samukawa *et al.*, 2014). Using AZA we observed a decreased affinity for DIC, with kinetics very similar to those of cells growing at 20 000 ppm, underlining the important role that extracellular CA plays in this CCM. As far as we are aware, there is no literature for aquatic (or terrestrial) photoautotrophs with C_4 metabolism relying on eCA. On the contrary, work by Reiskind *et al.* (1988) on the CCM in the marine green macroalgae *Udotea flabellum*, which has a C_4 fixation pathway based on PEP carboxykinase, showed that CA was not involved, as the CCM was active in the presence of a CA inhibitor. Furthermore, although the model of Kustka *et al.* (2014) reported up-regulation of a number of carbonic anhydrases, including CA-6 that could be located at the cell surface, in their model (Fig. 6) they located it in the chloroplast endoplasmic reticulum. However, although there is no experimental evidence for eCA being involved in C_4 metabolism, and most interpretations of CA increases are linked to the operation of a biophysical CCM, it is theoretically possible that an eCA could facilitate the rate of inward diffusion of either CO_2 or HCO_3^-, or both.

As has been found for higher plant Rubisco (Lorimer *et al.*, 1976), we observed an increase of Rubisco activity upon CO_2 activation, presumably linked to a change in Rubisco carbamylation state, which was threefold for cells grown at 400 and 20 000 ppm CO_2. Rubisco activity, whether the enzyme was activated or not, was always higher at high vs low CO_2, on a Chl*a* basis. It is possible that the greater Rubisco activity at high CO_2 increased the capacity to fix CO_2, as there appears to be little excess carboxylation capacity in diatoms (Glover & Morris, 1979).

Evidence for and against C_4 metabolism in *Thalassiosira pseudonana*

Whether or not C_4 photosynthesis is involved in any of the kinetic characteristics that have been observed in *T. pseudonana* has been a matter of debate. Kustka *et al.* (2014) produced a model of C_4 metabolism for *T. pseudonana* in which PEPC, in the chloroplastic endoplasmic reticulum or the periplastidic space, fixes HCO_3^- to produce oxaloacetic acid that is transported to the chloroplast where it is decarboxylated by pyruvate carboxylase to produce CO_2 in the vicinity of Rubisco.

In our experiments, the activity of PEPC was lower in cells from low CO_2 (grown at 400 or switched to 50 ppm) than in those from high CO_2 (20 000 ppm): the opposite of what is expected for C_4 metabolism. The ratio of PEPC : Rubisco was also lower at 400 than at 20 000 ppm and decreased with time when cells were switched from 20 000 to 50 ppm. Furthermore, the ratio of PEPC : Rubisco in *T. pseudonana* was always much less than 1, while in aquatic C_4 plants it is between 1.8 and 6.6, and in terrestrial plants it is more than 5 (Zhang *et al.*, 2014). Moreover, the activity of other enzymes required for the operation of the C_4 cycle, such as PPDK, was also lower at low CO_2. Although NAD-ME, one of the three possible decarboxylating C_4 enzymes, had a fourfold higher activity at 400 than at 20 000 ppm, this enzyme also contributes to the overall regulation of malate metabolism in many organisms and thus its

increase in activity is not necessarily associated with C_4 metabolism. Malate is an important substrate for mitochondria, and a significant fraction of glycolytic products enter the Krebs cycle via the combined action of PEPC, malate dehydrogenase, and malic enzyme without any link to C_4 metabolism. Recently it has been shown that NAD-ME is located within the mitochondria in *P. tricornutum* (Xue *et al.*, 2015) and within the cytosol in *T. pseudonana* (Tanaka *et al.*, 2014). This suggests that the CO_2 released from this decarboxylation would not be in the vicinity of Rubisco. Overall, these enzyme activities, and their pattern of change, are inconsistent with the operation of C_4 photosynthesis in this species.

The conclusion that C_4 metabolism is not an important component of the CCM in *T. pseudonana* is in agreement with recent work of Tanaka *et al.* (2014), who observed a greater abundance of PEPC1 and PEPC2 transcripts in high than in low CO_2. Similarly, the transcripts for other enzymes potentially involved in C_4 photosynthesis, phosphoenolpyruvate carboxykinase (PEPCK), PPDK and NAD-ME, were not higher when *T. pseudonana* was grown in low vs high CO_2, nor were they regulated by the circadian cycle, suggesting that they are not involved in C_4 photosynthesis. The absence of C_4 metabolism was also concluded from the lack of change in PEPC : Rubisco ratio in cells of *T. pseudonana* grown at 50 or 800 ppm (Trimborn *et al.*, 2009). Finally, pulse-chase experiments showed that *T. pseudonana* did not incorporate 4-carbon molecules during photosynthesis and immunoblots showed no difference in PEPC abundance in cells grown at 380 or 100 ppm (Roberts *et al.*, 2007b). By contrast, the addition of 3,3-dichloro-2-(dihydroxyphosphinoylmethyl)-propenoate (DCDP), an inhibitor of PEPC, or 3-mercaptopicolinic acid (3-MPA), an inhibitor of PEPCK, reduced photosynthetic activity in *T. pseudonana* (McGinn & Morel, 2008). However, it has subsequently been shown that both inhibitors had no effect on the half-saturation constant, but instead inhibited V_{max}, suggesting that they had a general toxic effect on metabolism rather than a specific effect on the CCM (Tanaka *et al.*, 2005, 2014). The reason for these different conclusions is currently unclear. Kustka *et al.* (2014) reported rapid (within 30 min) but transient (returned close to pretransient levels in 90 min) changes in two forms of PEPC transcripts on transfer from pH 7.61 to 8.48. An alternative explanation to PEPC playing a photosynthetic role is that the response is linked to internal pH homeostasis by the production of carboxylic acids. Haimovich-Dayan *et al.* (2013) concluded that *P. tricornutum* lacked C_4 metabolism and proposed that any C_4-like metabolism is a futile cycle to dissipate light energy rather than to fix carbon and may also play a role in internal pH homeostasis. Although diatoms such as *T. pseudonana* have biophysical pH regulation mechanisms based on a Na^+-energized plasmalemma (Taylor *et al.*, 2012), a biochemical pH-stat based on PEPC as part of the glycolytic pathway may also be involved in pH regulation (Sakano, 1998). The steady-state up-regulation of PEPC reported by Kustka *et al.* (2014) of between 1.52- and 1.75-fold is much lower than for the different forms of CA whose protein-level up-regulation is in broad agreement with our changes in activity. Kustka *et al.* (2014) also reported an up-regulation of two forms of the anion channel Bestrophin (Hartzell *et al.*, 2008) of between 3.31- and 4.24-fold, which could be involved in facilitating diffusion of oxaloacetate into the chloroplast. However, Bestrophin can also act as an HCO_3^- channel (Qu & Hartzell, 2008), which would also be consistent with a biophysically based CCM.

Acknowledgements

R.C.'s studentship was supported by the Ministère de l'Education Nationale, de la Recherche et de la Technologie (MENRT). Financial support was provided by CNRS, Aix Marseille Université, the Region PACA, IBiSA and A*MIDEX project (no. ANR-11-IDEX-0001-02) (B.G.) and the UK Natural Environment Research Council (S.C.M.). We thank Ahmed Zellat for technical support.

Author contributions

R.C., S.C.M. and B.G. planned and designed the research. R.C. and L.D. performed the experiments. R.C., S.C.M. and B.G. analysed the data and wrote the manuscript.

References

Allen AE, Dupont CL, Obornik M, Horak A, Nunes-Nesi A, McCrow JP, Zheng H, Johnson DA, Hu H, Fernie AR *et al.* 2011. Evolution and metabolic significance of the urea cycle in photosynthetic diatoms. *Nature* **473**: 203–207.

Armbrust EV. 2009. The life of diatoms in the world's oceans. *Nature* **459**: 185–192.

Armbrust EV, Berges JA, Bowler C, Green BR, Martinez D, Putnam NH, Zhou S, Allen AE, Apt KE, Bechner M *et al.* 2004. The genome of the diatom *Thalassiosira pseudonana*: ecology, evolution, and metabolism. *Science* **306**: 79–86.

Badger MR, Andrews TJ, Whitney SM, Ludwig M, Yellowlees DC, Leggat W, Price GD. 1998. The diversity and coevolution of Rubisco, plastids, pyrenoids, and chloroplast-based CO_2-concentrating mechanisms in algae. *Canadian Journal of Botany* **76**: 1052–1071.

Bowes G, Ogren WL, Hageman RH. 1971. Phosphoglycolate production catalyzed by ribulose diphosphate carboxylase. *Biochemical and Biophysical Research Communications* **45**: 716–722.

Bowler C, Allen AE, Badger JH, Grimwood J, Jabbari K, Kuo A, Maheswari U, Martens C, Maumus F, Otillar RP *et al.* 2008. The *Phaeodactylum* genome reveals the evolutionary history of diatom genomes. *Nature* **456**: 239–244.

Bradford MM. 1976. A rapid and sensitive method for the quantitation of microgram quantities of protein utilizing the principle of protein-dye binding. *Analytical Biochemistry* **72**: 248–254.

Burkhardt S, Amoroso G, Riebesell U, Sültemeyer D. 2001. CO_2 and HCO_3^- uptake in marine diatoms acclimated to different CO_2 concentrations. *Limnology and Oceanography* **46**: 1378–1391.

Clark DR, Flynn KJ. 2000. The relationship between the dissolved inorganic carbon concentration and growth rate in marine phytoplankton. *Proceedings of the Royal Society of London B: Biological Sciences* **267**: 953–959.

Crawfurd KJ, Raven JA, Wheeler GL, Baxter EJ, Joint I. 2011. The response of *Thalassiosira pseudonana* to long-term exposure to increased CO_2 and decreased pH. *PLoS ONE* **6**: e26695.

Deschamps P, Moreira D. 2012. Reevaluating the green contribution to diatom genomes. *Genome Biology and Evolution* **4**: 795–800.

Erales J, Gontero B, Maberly SC. 2008. Specificity and function of glyceraldehyde-3-phosphate dehydrogenase in a freshwater diatom, *Asterionella formosa* (Bacillariophyceae). *Journal of Phycology* **44**: 1455–1464.

Falkowski PG, Katz ME, Knoll AH, Quigg A, Raven JA, Schofield O, Taylor FJR. 2004. The evolution of modern eukaryotic phytoplankton. *Science* **305**: 354–360.

Glover HE, Morris I. 1979. Photosynthetic carboxylating enzymes in marine phytoplankton. *Limnology and Oceanography* **24**: 510–519.

Gontero B, Salvucci ME. 2014. Regulation of photosynthetic carbon metabolism in aquatic and terrestrial organisms by Rubisco activase, redox-modulation and CP12. *Aquatic Botany* **118**: 14–23.

Goyet C, Poisson A. 1989. New determination of carbonic acid dissociation constants in seawater as a function of temperature and salinity. *Deep Sea Research Part A. Oceanographic Research Papers* **36**: 1635–1654.

Haimovich-Dayan M, Garfinkel N, Ewe D, Marcus Y, Gruber A, Wagner H, Kroth PG, Kaplan A. 2013. The role of C_4 metabolism in the marine diatom *Phaeodactylum tricornutum*. *New Phytologist* **197**: 177–185.

Harada H, Nakatsuma D, Ishida M, Matsuda Y. 2005. Regulation of the expression of intracellular beta-carbonic anhydrase in response to CO_2 and light in the marine diatom *Phaeodactylum tricornutum*. *Plant Physiology* **139**: 1041–1050.

Hartzell HC, Qu Z, Yu K, Xiao Q, Chien L-T. 2008. Molecular physiology of bestrophins: multifunctional membrane proteins linked to best disease and other retinopathies. *Physiological Reviews* **88**: 639–672.

Hopkinson BM, Dupont CL, Allen AE, Morel FMM. 2011. Efficiency of the CO_2-concentrating mechanism of diatoms. *Proceedings of the National Academy of Sciences, USA* **108**: 3830–3837.

Hopkinson BM, Meile C, Shen C. 2013. Quantification of extracellular carbonic anhydrase activity in two marine diatoms and investigation of its role. *Plant Physiology* **162**: 1142–1152.

Katz ME, Wright JD, Miller KG, Cramer BS, Fennel K, Falkowski PG. 2005. Biological overprint of the geological carbon cycle. *Marine Geology* **217**: 323–338.

Kikutani S, Tanaka R, Yamazaki Y, Hara S, Hisabori T, Kroth PG, Matsuda Y. 2012. Redox regulation of carbonic anhydrases via thioredoxin in chloroplast of the marine diatom *Phaeodactylum tricornutum*. *Journal of Biological Chemistry* **287**: 20689–20700.

Kroth PG. 2015. The biodiversity of carbon assimilation. *Journal of Plant Physiology* **172**: 76–81.

Kustka AB, Milligan AJ, Zheng H, New AM, Gates C, Bidle KD, Reinfelder JR. 2014. Low CO_2 results in a rearrangement of carbon metabolism to support C_4 photosynthetic carbon assimilation in *Thalassiosira pseudonana*. *New Phytologist* **204**: 507–520.

Lara MV, Casati P, Andreo CS. 2002. CO_2-concentrating mechanisms in *Egeria densa*, a submersed aquatic plant. *Physiologia Plantarum* **115**: 487–495.

Lorimer GH, Badger MR, Andrews TJ. 1976. The activation of ribulose-1,5-bisphosphate carboxylase by carbon dioxide and magnesium ions. Equilibria, kinetics, a suggested mechanism, and physiological implications. *Biochemistry* **15**: 529–536.

Magnin NC, Cooley BA, Reiskind JB, Bowes G. 1997. Regulation and localization of key enzymes during the Induction of Kranz-less, C_4-type photosynthesis in *Hydrilla verticillata*. *Plant Physiology* **115**: 1681–1689.

Mann DG, Vanormelingen P. 2013. An inordinate fondness? The number, distributions, and origins of diatom species. *Journal of Eukaryotic Microbiology* **60**: 414–420.

Matsuda Y, Nakajima K, Tachibana M. 2011. Recent progresses on the genetic basis of the regulation of CO_2 acquisition systems in response to CO_2 concentration. *Photosynthesis Research* **109**: 191–203.

McGinn PJ, Morel FMM. 2008. Expression and inhibition of the carboxylating and decarboxylating enzymes in the photosynthetic C_4 pathway of marine diatoms. *Plant Physiology* **146**: 300–309.

Mekhalfi M, Puppo C, Avilan L, Lebrun R, Mansuelle P, Maberly SC, Gontero B. 2014. Glyceraldehyde-3-phosphate dehydrogenase is regulated by ferredoxin-NADP reductase in the diatom *Asterionella formosa*. *New Phytologist* **203**: 414–423.

Moustafa A, Beszteri B, Maier UG, Bowler C, Valentin K, Bhattacharya D. 2009. Genomic footprints of a cryptic plastid endosymbiosis in diatoms. *Science* **324**: 1724–1726.

Mueller-Cajar O, Stotz M, Wendler P, Hartl FU, Bracher A, Hayer-Hartl M. 2011. Structure and function of the AAA+ protein CbbX, a red-type Rubisco activase. *Nature* **479**: 194–199.

Nakajima K, Tanaka A, Matsuda Y. 2013. SLC4 family transporters in a marine diatom directly pump bicarbonate from seawater. *Proceedings of the National Academy of Sciences, USA* **110**: 1767–1772.

Qu Z, Hartzell HC. 2008. Bestrophin Cl^- channels are highly permeable to HCO_3. *American Journal of Physiology–Cell Physiology* **294**: C1371–C1377.

Raven J. 2010. Inorganic carbon acquisition by eukaryotic algae: four current questions. *Photosynthesis Research* **106**: 123–134.

Raven JA, Giordano M, Beardall J, Maberly SC. 2012. Algal evolution in relation to atmospheric CO_2: carboxylases, carbon-concentrating mechanisms and carbon oxidation cycles. *Philosophical Transactions of the Royal Society B: Biological Sciences* **367**: 493–507.

Reinfelder JR, Kraepiel AML, Morel FMM. 2000. Unicellular C_4 photosynthesis in a marine diatom. *Nature* **407**: 996–999.

Reinfelder JR, Milligan AJ, Morel FMM. 2004. The role of the C_4 pathway in carbon accumulation and fixation in a marine diatom. *Plant Physiology* **135**: 2106–2111.

Reiskind JB, Bowes G. 1991. The role of phosphoenolpyruvate carboxykinase in a marine macroalga with C_4-like photosynthetic characteristics. *Proceedings of the National Academy of Sciences, USA* **88**: 2883–2887.

Reiskind JB, Seamon PT, Bowes G. 1988. Alternative methods of photosynthetic carbon assimilation in marine macroalgae. *Plant Physiology* **87**: 686–692.

Ritchie R. 2006. Consistent sets of spectrophotometric chlorophyll equations for acetone, methanol and ethanol solvents. *Photosynthesis Research* **89**: 27–41.

Roberts K, Granum E, Leegood R, Raven J. 2007a. Carbon acquisition by diatoms. *Photosynthesis Research* **93**: 79–88.

Roberts K, Granum E, Leegood RC, Raven JA. 2007b. C_3 and C_4 pathways of photosynthetic carbon assimilation in marine diatoms are under genetic, not environmental, control. *Plant Physiology* **145**: 230–235.

Sage RF. 2004. The evolution of C_4 photosynthesis. *New Phytologist* **161**: 341–370.

Sakano K. 1998. Revision of biochemical pH-stat: involvement of alternative pathway metabolisms. *Plant and Cell Physiology* **39**: 467–473.

Samukawa M, Shen C, Hopkinson B, Matsuda Y. 2014. Localization of putative carbonic anhydrases in the marine diatom, *Thalassiosira pseudonana*. *Photosynthesis Research* **121**: 235–249.

Sarthou G, Timmermans KR, Blain S, Tréguer P. 2005. Growth physiology and fate of diatoms in the ocean: a review. *Journal of Sea Research* **53**: 25–42.

Sims PA, Mann DG, Medlin LK. 2006. Evolution of the diatoms: insights from fossil, biological and molecular data. *Phycologia* **45**: 361–402.

Sorhannus U. 2007. A nuclear-encoded small-subunit ribosomal RNA timescale for diatom evolution. *Marine Micropaleontology* **65**: 1–12.

Spilling K, Ylostalo P, Simis S, Seppala J. 2015. Interaction effects of light, temperature and nutrient limitations (N, P and Si) on growth, stoichiometry and photosynthetic parameters of the cold-water diatom *Chaetoceros wighamii*. *PLoS ONE* **10**: e0126308.

Sültemeyer D, Klöck G, Kreuzberg K, Fock H. 1988. Photosynthesis and apparent affinity for dissolved inorganic carbon by cells and chloroplasts of *Chlamydomonas reinhardtii* grown at high and low CO_2 concentrations. *Planta* **176**: 256–260.

Tanaka R, Kikutani S, Mahardika A, Matsuda Y. 2014. Localization of enzymes relating to C_4 organic acid metabolisms in the marine diatom, *Thalassiosira pseudonana*. *Photosynthesis Research* **121**: 251–263.

Tanaka Y, Nakatsuma D, Harada H, Ishida M, Matsuda Y. 2005. Localization of soluble β-carbonic anhydrase in the marine diatom *Phaeodactylum tricornutum*. Sorting to the chloroplast and cluster formation on the girdle lamellae. *Plant Physiology* **138**: 207–217.

Taylor AR, Brownlee C, Wheeler GL. 2012. Proton channels in algae: reasons to be excited. *Trends in Plant Science* **17**: 675–684.

Trimborn S, Wolf-Gladrow D, Richter K-U, Rost B. 2009. The effect of pCO_2 on carbon acquisition and intracellular assimilation in four marine diatoms. *Journal of Experimental Marine Biology and Ecology* **376**: 26–36.

Voznesenskaya EV, Franceschi VR, Kiirats O, Freitag H, Edwards GE. 2001. Kranz anatomy is not essential for terrestrial C_4 plant photosynthesis. *Nature* **414**: 543–546.

Weiss RF. 1974. Carbon dioxide in water and seawater: the solubility of a non-ideal gas. *Marine Chemistry* **2**: 203–215.

Whitney SM, Sharwood RE, Orr D, White SJ, Alonso H, Galmés J. 2011. Isoleucine 309 acts as a C_4 catalytic switch that increases ribulose-1,5-bisphosphate carboxylase/oxygenase (rubisco) carboxylation rate in *Flaveria*. *Proceedings of the National Academy of Sciences, USA* **108**: 14688–14693.

Wilbur KM, Anderson NG. 1948. Electrometric and colorimetric determination of carbonic anhydrase. *Journal of Biological Chemistry* **176**: 147–154.

Xu J, Zhang X, Ye N, Zheng Z, Mou S, Dong M, Xu D, Miao J. 2013. Activities of principal photosynthetic enzymes in green macroalga *Ulva linza*: functional implication of C_4 pathway in CO_2 assimilation. *Science China Life Sciences* **56**: 571–580.

Xue J, Niu YF, Huang T, Yang WD, Liu JS, Li HY. 2015. Genetic improvement of the microalga *Phaeodactylum tricornutum* for boosting neutral lipid accumulation. *Metabolic Engineering* **27**: 1–9.

Zhang Y, Yin L, Jiang H-S, Li W, Gontero B, Maberly SC. 2014. Biochemical and biophysical CO_2 concentrating mechanisms in two species of freshwater macrophyte within the genus *Ottelia* (Hydrocharitaceae). *Photosynthesis Research* **121**: 285–297.